

## Comparative Study of Hydrogen Adsorption in Slit-like Pores of Carbon Adsorbents and on Fullerene Molecules

V.M. Samsonov, V.V. Zubkov, I.V. Grinev

*Departments of General and Theoretical Physics, Tver State University, Tver 170002, Russian Federation*

(Received 20 May 2013; revised manuscript received 05 July 2013; published online 31 August 2013)

Adsorption of hydrogen in slit-like pores of carbon adsorbents and on fullerene molecules was investigated using the classical density functional theory. Hydrogen adsorption in a gap between two graphene walls was calculated at different temperatures and pressures. The obtained results agree with the data found using the Dubinin theory of the volume pore filling and with the available molecular dynamics results. It has been shown that conventional carbon adsorbents corresponding to the slit-like model and fullerene materials should have approximately equal storage capacities. However, such a capacity is sufficient for practical storage and use of hydrogen at low temperatures only (at about 20 K), and at room temperatures some special active sites of adsorption should be used to solve the problem under consideration.

**Keywords:** Adsorption, Hydrogen, Nanopore, Slit-like pore, Fullerenes, Density functional theory.

PACS numbers: 68.18.Fg, 68.43.De

Hydrogen adsorbed layers in conventional porous carbon materials, and on fullerene molecules and in fullerene materials are of the great interest in view of further development of the hydrogen energetics. From ecological point of view, it may be treated as a very clear way of the production and consumption of energy. Being the most abundant element on the Earth, hydrogen seems to be most promising fuel having the lowest molecular weight and the highest combustion temperature. A secondary, but an important problem is its storage, and according to estimations [1], 3.1 kg of the molecular hydrogen is sufficient for the 500 km car mileage. The existing methods of the hydrogen concentration [1], including the liquefaction, storing at high pressures, using hydrides of metals and alloys, can not solve the problem completely. The compressed gas really may be treated as one of main alternatives to liquid and liquefied fuels, but it requires unacceptably high storage pressures.

At same time, a number of results [2-7] indicate that physical adsorption may be regarded as a promising method of the hydrogen storage. In recent years, hopes to increase the adsorption of hydrogen were associated with using single-walled carbon nanotubes (SWNTs) [1], carbon nanofibers, and fullerenes [4, 7]. Molecular modeling of the hydrogen adsorption by the Monte Carlo on SWNTs stacked bunches with different spacings between tubes (at 77 and 293 K and pressures up to 20 MPa) also demonstrates the high adsorption activity of such structures [5, 6]. However, the simulation results for hydrogen adsorption in carbon adsorbents do not allow to make an unambiguous conclusions about prospects of their application.

The hydrogen adsorption on different highly developed surfaces of activated carbons has been measured at different temperature and pressure [8], and the slit-pore model of some width  $H$  is usually used. Usually models of adsorption in pores are based on Dubinin-Radushkevich and Dubinin-Astakhov

approaches [9, 10], the Langmuir isotherm, and a more recent vacancy solution theory formulation [11]. Among the molecular modeling, the density functional theory [12, 13], and molecular simulation techniques [7, 14, 15] are of also promising.

Density functional theory (DFT) may be regarded as a modern powerful method for the investigation of vapor-liquid interfaces, adsorption in pores, and calculations of pore size distributions from experimental isotherms [16]. However, a detailed comparison of DFT results with experiment data is not straightforward. Structural and energetic heterogeneity of pores strongly influences on the adsorption in real materials [17, 18]. The ways of measurements are often different and, therefore, the experimental results, as a rule, contradicts to each other [19].

In frames of the slit-like pore model, the formation of micropores in carbon adsorbents is considered as a process of thermochemical elimination of atoms from hexagonal planes in carbon crystallites when being activated by water vapors [20]. In our calculations we have used the model of the ideal slit-like pore, for which the distance between the surfaces corresponds to 3-5 removed layers of graphene. The neighboring micropores are separated with a single carbon monolayer. We assume that the distance between hexagonal layers in graphite is equal to 0.335 nm and the length of the hexagons is 0.142 nm. Adsorbate molecule, located in the pore undergoes adsorptive forces of two planes (below referred to as upper and lower). The influence of the side walls is much smaller and, respectively, may be neglected [21]. The potential of the interaction between a hydrogen molecule and the carbon atom on the graphite wall may be presented as:

$$U_{sf}(z) = 2\pi\rho_s\varepsilon_{sf}\sigma_{sf}^2 \left( \frac{2}{5} \frac{\sigma_{sf}^{10}}{z^{10}} - \frac{\sigma_{sf}^4}{z^4} \right), \quad (1)$$

where  $\rho_s$  is the wall surface density, i.e. the number of

atoms per unit area,  $\sigma_{sf}$  and  $\varepsilon_{sf}$  are the parameters of the wall-fluid potential. The wall-fluid parameters  $\sigma_{sf}$  and  $\varepsilon_{sf}$  may be estimated using the Lorentz-Berthelot mixing rules  $\sigma_{sf} = (\sigma_s + \sigma_f)/2$ ,  $\varepsilon_{sf} = \sqrt{\varepsilon_s \varepsilon_f}$  and values of  $\sigma$  and  $\varepsilon$  parameters for solid (subscript  $s$ ) and fluid (subscript  $f$ ). The reduced surface density of atoms in the walls of graphite may be evaluated as follows

$$n_s = \rho_s \sigma_s^2 = \frac{N_s}{S} \sigma_s^2 = \frac{2\sigma_s^2}{Sb^2} = 2 \left( \frac{\sigma_s}{b} \right)^2 \frac{b^2}{S} = 4.413. \quad (2)$$

The total potential of the pore walls

$$U(z) = U_{sf}(z) + U_{sf}(H-z), \quad (3)$$

is equal to the sum of two terms corresponding to two walls located at  $z=0$  and  $z=H$  respectively ( $z$  - axe is normal to the pore walls).

The main problem of DFT is constructing characteristic functions (the Helmholtz energy  $F[\rho(\mathbf{r})]$  and the grand potential  $\Omega[\rho(\mathbf{r})]$ ) as the density functionals [16]:

$$F_{id}[\rho(\mathbf{r})] = kT \int d^3\mathbf{r} \rho(\mathbf{r}) [\ln \rho(\mathbf{r}) - 1], \quad (4)$$

$$\Omega[\rho(\mathbf{r})] = F[\rho(\mathbf{r})] + \int [U(\mathbf{r}) - \mu] \rho(\mathbf{r}) d^3\mathbf{r}, \quad (5)$$

where  $U(\mathbf{r})$  is the external potential of the pore walls,  $\mu$  is the chemical potential. The Helmholtz energy was written here as the ideal-gas term, and the excess term can be decomposed in the hard-sphere (subscript  $hs$ ) and attractive (subscript  $att$ ) terms:

$$F_{ex}[\rho(\mathbf{r})] = F_{hs}[\rho(\mathbf{r})] + F_{att}[\rho(\mathbf{r})]. \quad (6)$$

In turn, the excess Helmholtz energy due to the hard sphere repulsion  $F_{hs}[\rho(\mathbf{r})]$  may be presented using the modified fundamental measure theory (MFMT) [24]:

$$F_{hs}[\rho(\mathbf{r})] = kT \int \Phi^{hs} [n_\alpha(\mathbf{r})] d^3\mathbf{r}. \quad (7)$$

In (7) the reduced excess energy density  $\Phi^{hs}$  is presented as a function of six weighted densities  $n_i(\mathbf{r}) = \int \rho(\mathbf{r}') \omega^{(i)}(|\mathbf{r}-\mathbf{r}'|) d^3\mathbf{r}'$ . The attractive part of the excess Helmholtz energy can be written in frames of the mean-field approximation

$$F_{att} = \frac{1}{2} \iint d\mathbf{r}' d\mathbf{r} u^{att}(|\mathbf{r}-\mathbf{r}'|) \rho(\mathbf{r}) \rho(\mathbf{r}'). \quad (8)$$

In Eq. (8)  $u^{att}$  is the long-range attractive part of L<sub>J</sub> potential represented according WCA potential model [25]. The minimization of the grand potential with respect to the density profiles yields the following Euler-Lagrange equation:

$$\rho(\mathbf{r}) = \exp \left[ \beta\mu - \beta U(\mathbf{r}) - \beta \frac{\delta F[\rho(\mathbf{r})]}{\delta \rho(\mathbf{r})} \right]. \quad (9)$$

Below we will use the reduced local density  $\eta = \pi d_f^3 \rho / 6$  - where  $d_f$  is the hard sphere diameter of the hydrogen molecule which can be expressed through  $\sigma_f$  [26]:

$$d_f = \frac{1 + 0.2977 kT / \varepsilon_f}{1 + 0.33163 kT / \varepsilon_f + 1.0477 \times 10^{-3} (kT / \varepsilon_f)^2} \sigma_f. \quad (10)$$

Knowing the density profile  $\rho(z)$  one can find the reduced absolute adsorption

$$\Gamma^* = \int_0^H \eta(z) dz \quad (11)$$

in the pore in question. Below two commonly used variables: the adsorption of hydrogen

$$a = \frac{6}{\pi} \left( \frac{\sigma_s}{d} \right)^2 \frac{\Gamma^*}{M_s \rho_s \sigma_s^2}$$

in mmol/g and the gravimetric density of  $H_2$  (%)  $wt = 100\% / (1 + 1/(aM_f))$  are calculated. Here  $M_s$  and  $M_f$  are molecular masses of graphite and hydrogen respectively,  $m_f$  is the total mass of hydrogen in the pore,  $m_s$  is the mass of the pore interpreted as the total mass of two walls.

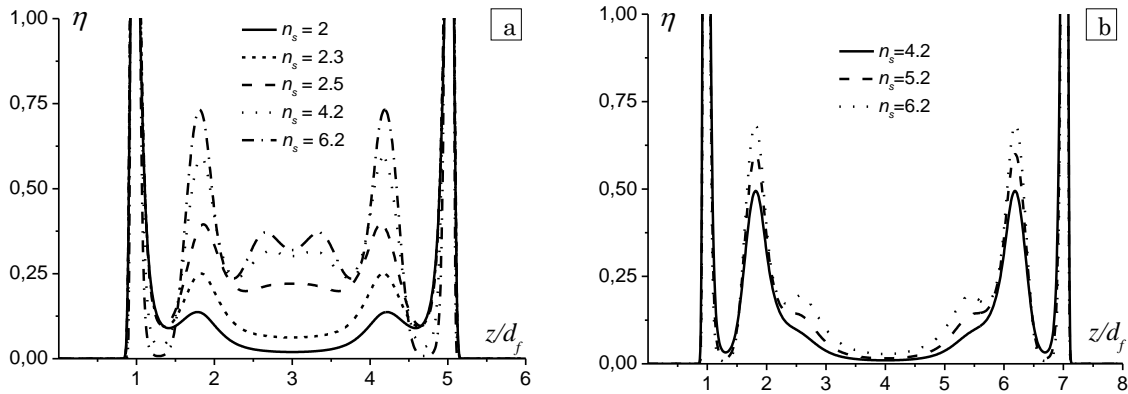
We have calculated the density profiles corresponding to different values of the wall parameters in a wide range of the wall surface density  $n_s$  (from 2.0 to 6.2). It is noteworthy that an intermediate value  $n_s = 4.4$  corresponds to real porous graphite adsorbents [20]. The profiles in question, corresponding to the pore width  $H = 6d_f$  are presented in Fig. 1a. One can see that the wall density variation affects drastically on the profile form. Really, for  $n_s \leq 2.0$  the density profiles corresponds to profiles of two single walls of the same surface density. The force fields have been overlapped for  $n_s = 2.3$ . This results in the growth of the adsorbate density in the central area of the pore and the formation of a weak central maximum. At the surface density  $n_s = 2.5$  in the central plateau seems to be formed. The further growth of the wall density yields two weak central maxima. It is remarkable that this effect begins to be developed just for the value of the surface wall density corresponding to the real porous graphite material. At higher values of the wall density all the maxima in question are growing. An increasing of the pore width results in a diminishing and gradual disappearance of the central maximum (Fig. 1b).

Fig. 2 presents subcritical adsorbate density profiles corresponding to the pore width  $H = 8d_f$  and different values of the vapor pressure  $p < p_{sat}$ . One can see that

at low pressures ( $p/p_{sat} \leq 0.3$ ) the pressure variation does not influence significantly on the form of the density profiles. At high pressures ( $p/p_{sat} \geq 0.6$ ) the density in the central part of the pore corresponds to a liquid-like state. Besides it is worth to mention that for this value of the pore width and high vapor pressure one can observe 8 maxima of the density profile.

In view of experimental results [20], the slit-like pore model investigated in this work is the most adequate to the adsorption of hydrogen in real porous

graphites. We have calculated the density profiles for hydrogen adsorbed in pores of different widths. Corresponding averaged results are presented in Table 1. The pore width 1.36 nm (Fig. 3a), corresponds to 4 burnt graphene monolayers. The results presented in this figure were obtained for subcritical temperature  $T = 20.38K$ . One can observe two pronounced maxima near the pore walls and two weak maxima at the center of the pore. In the pore center itself a minimum is formed.



**Fig. 1** – Reduced density profiles of Lennard-Jones fluid in a slit-like pore at temperature  $T = 0.75T_c$ ,  $\sigma_s/\sigma_f = 0.9$ ,  $\varepsilon_s/\varepsilon_f = 1.2$ ,  $p = 0.25p_{sat}$  and different densities of adsorbate: (a) pore width  $H = 6d_f$ , (b) pore width  $H = 8d_f$

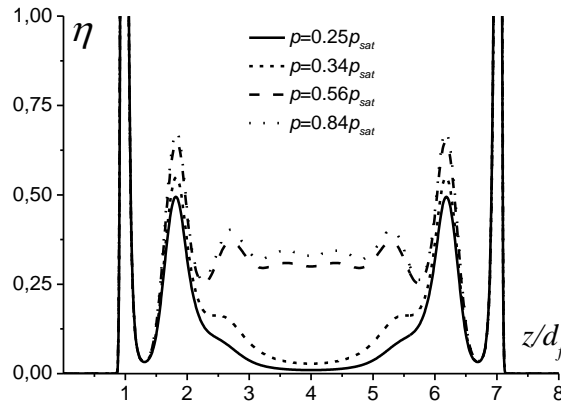


**Fig. 2** – Reduced density profiles of Lennard-Jones fluid in a slit-like pore at temperature  $T = 0.75T_c$ , pore width  $H = 8d_f$ ,  $\sigma_s/\sigma_f = 0.9$ ,  $\varepsilon_s/\varepsilon_f = 1.2$ ,  $n_s = 4.2$ , and different pressures

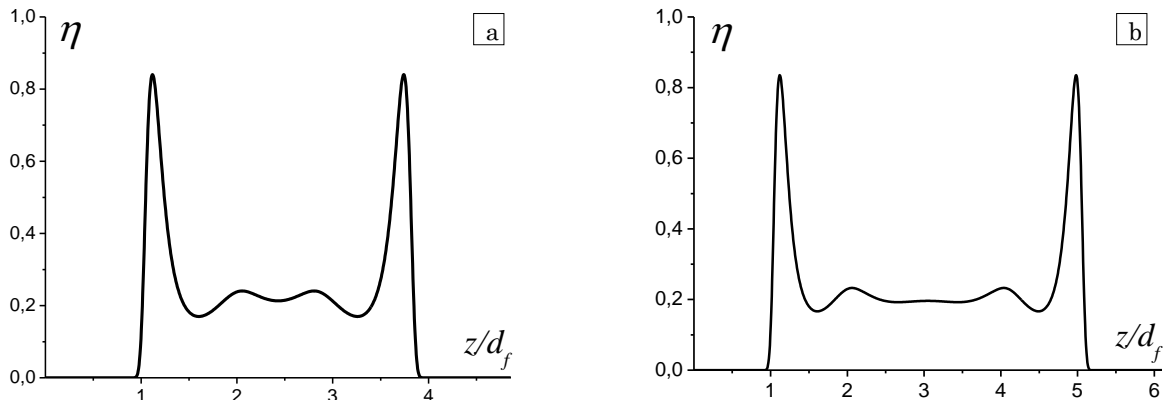


**Fig. 3** – Reduced density profiles of hydrogen in a slitlike pore at temperature  $T = 77K$ , pressure  $p = 20$  MPa: (a) pore width  $H = 1.36$  nm,  $\Gamma^* = 45.75$ ,  $wt = 8.38$ , (b) pore width  $H = 1.7$  nm,  $\Gamma^* = 57.97$ ,  $wt = 10.39$

**Table 1** – The adsorption of hydrogen in a modeling slit-like pore, according to the Dubinin theory of the volume pore filling and DFT

	20.38 K, 20 kPa		77 K, 20 MPa		200 K, 20 MPa	
	[1]	Present paper	[1]	Present paper	[1]	Present paper
Adsorption, mmol/g	56.64	62.73	53.5	51.86	46.6	27.68
Gravimetric density in H <sub>2</sub> (%)	11.3	11.3	10.7	9.39	9.3	5.25

Following to [20] we have calculated density profiles for a supercritical temperature  $T = 77$  K and a high enough pressure  $p = 20$  MPa of the gaseous hydrogen. Fig. 3 presents the results on the density profiles in slit-like pores, corresponding to 4 (Fig. 3a) and 5 (Fig. 3b) deleted graphene monolayer, respectively. One can see that for these pore widths the density profiles seem to be more similar than the profiles presented in Fig. 3. In the case under consideration we have a weak central minimum (Fig. 3a) or a plateau (Fig. 3b). For the chosen values of  $H$  the calculation results for  $\Gamma^*$  and  $wt$  presented in Table 1 are in very good agreement with the results presented in [20].

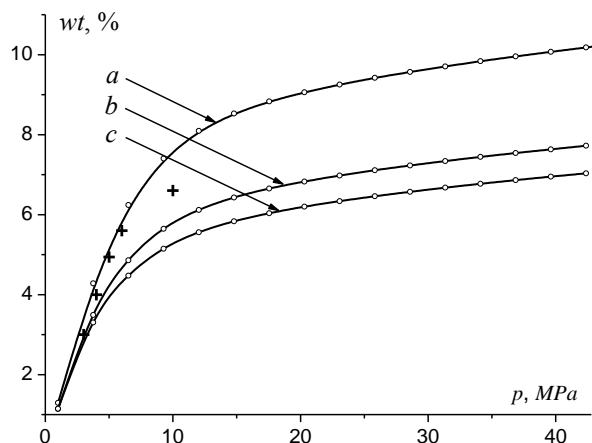


**Fig. 4** – Gravimetric density of hydrogen on  $C_{60}$  (a),  $C_{240}$  (b) и  $C_{540}$  (c) при  $T = 77$  K. Crosses in the Figure correspond to data [29]

For very high (room) temperatures (particularly for  $T = 200$  K) our calculation results are about twice underestimated in comparison with the results of paper [20]. As was mentioned above, the data [20] are

semiempirical, i.e. they were obtained combining standard experimental data for benzene with the Dubinin-Radushkevich phenomenological theory. As for high temperatures the quantum effects and the effects of non-ideality should be less pronounced, the data obtained in [20] seem to be more reliable.

Recently we applied the DFT-method to calculate the adsorption on outer and inner sides of 2D spherical adsorbents. Such a modeling system is adequate to fullerene molecules. According to Fig. 3, fullerene molecules demonstrate approximately the same adsorption capacity as the conventional carbon adsorption.

So, the results of our calculations carried out within the DFT approach show that the adsorption of hydrogen in carbon adsorbents should be of order of 10 weight percents in both cases: in conventional porous graphite adsorbents and in fullerene materials. Separate fullerene molecules may be interpreted as simplest models of such materials. From this point of view, conventional industrial carbon adsorbents and their modifications seem to be more promising for the hydrogen storage. This result agrees with the available experimental data [27, 28] and the results of paper [20] and [29]. In principle the obtained values of  $wt$  makes it possible to design an adsorption element for the storage of hydrogen as a promising vehicular fuel. At the same time, these values of  $wt$  are low enough at room temperatures. Probably, some high-energy sites of primary adsorption on the surface of micropores may be used to increase the adsorption of hydrogen. However, corresponding calculations are beyond frames of this paper.

## ACKNOWLEDGMENT

Financial support of Russian Foundation for Basic Research is acknowledged (grant No. 13-03-00119).

## REFERENCES

1. A.C. Dillon, K.M. Jones, T.A. Bekkedahl, C.H. Kiang, D.S. Bethune, M.J. Heben, *Nature* **386**, 377 (1997).
2. S. Hynek, W. Fuller, J. Bentley, *Int. J. Hydrogen Energ.* **22**, 601 (1997).
3. C. Carpetis, W. Peschka, *Int. J. Hydrogen Energ.* **5**, 539 (1980).
4. A. Chambers, C. Park, R.T. Baker, N.M. Rodriguez, *J. Phys. Chem. B* **102**, 4253 (1998).
5. F. Darkrim, D. Levesque, *J. Chem. Phys.* **109**, 4981 (1998).
6. Y.F. Yin, T. Mays, B. McEnan, *Langmuir* **16**, 10521 (2000).
7. K. Murata, K. Kaneko, H. Kanoh, D. Kasuya, K. Takahashi, F. Kokai, M. Yudasaka, S. Iijima, *J. Phys. Chem. B* **106**, 11132 (2002).
8. A. Anson, J. Jagiello, J.B. Parra, M.L. Sanjuan, A.M. Benito, W.K. Maser, M.T. Martinez, *J. Phys. Chem. B* **108**, 15820 (2004).
9. M.M. Dubinin, *Physical Adsorption of Gases and Vapors in Micropores. Progress in surface and membrane. Sci.* **9**, 1 (New York: Acad. Press: 1975).
10. S. Ismadji, S.K. Bhatia, *Langmuir* **17**, 1488 (2001).
11. S.K. Bhatia, L.P. Ding, *AIChE J.* **47**, 2136 (2001).
12. A.V. Neimark, P.I. Ravikovitch, *Langmuir* **13**, 5148 (1997).
13. P.I. Ravikovitch, A. Vishnyakov, R. Russo, A.V. Neimark, *Langmuir* **16**, 2311 (2000).
14. A. Vishnyakov, P.I. Ravikovitch, A.V. Neimark, *Langmuir* **15**, 8736 (1999).
15. M. Rzepka, P. Lamp, M.A. de la Casa-Lillo, *J. Phys. Chem. B* **102**, 10894 (1998).
16. J. Wu, *AIChE J.* **52**, 1169 (2006).
17. S.K. Bhatia, *Langmuir* **18**, 6845 (2002).

18. T.X. Nguyen, S.K. Bhatia, *Langmuir* **20**, 3532 (2004).
19. B.V. Fenelonov, E.A. Ustinov, V.A. Yakovlev, Ch.N. Barnakov, M.S. Mel'gunov, *Kinet. Catal.* **48**, 599 (2007).
20. A.A. Fomkin, V.A. Sinitsyn, *Prot. Met.* **44**, 150 (2008).
21. A.A. Vanin, E.M. Piotrowskaya, E.N. Brodskaya, *Zh. Fiz. Khim.* **78**, 2064 (2004).
22. D.D. Do, *Adsorption Analysis: Equilibria and Kinetics* (London: Imperial College Press: 1998).
23. D.V. Matyushov, R. Schmid, *J. Chem. Phys.* **104**, 8627 (1996).
24. Y.-X. Yu, J. Wu, *J. Chem. Phys.* **117**, 10156 (2002).
25. D.J. Weeks, D. Chandler, H.C. Andersen, *J. Chem. Phys.* **54**, 5237 (1971).
26. Y. Tang, *J. Chem. Phys.* **116**, 6694 (2002).
27. R. Chahinea, T.K. Bose, *Int. J. Hydrogen Energ.* **19**, 161 (1994).
28. M.A. de la Casa-Lillo, F. Lamari-Darkrim, D. Cazorla-Amoro's, A. Linares-Solano, *J. Phys. Chem. B* **106**, 10930 (2002).
29. A.V. Vahruchev, M.V. Suetin, *Alternativnaya Energetika i Ekologia* **6**, 39 (2006).